Viruses, Molecular Biology of Tumor Viruses, R. Weiss, N. Teich, H. Varmus, J. Coffin, Eds. (Cold Spring Harbor Laboratory, Cold Spring Harbor, NY, ed. 2, 1985), pp. 249–356.
5. B. D. Miles and H. L. Robinson, *J. Virol.* **54**, 295 (1985).
6. S. P. Goff, E. Gilboa, O. N. Witte, D. Baltimore, *Cell* **22**, 777 (1980); H. E. Varmus, *Science* **216**, 812 (1982); R. Swanstrom, R. C. Parker, H. E. Varmus, J. M. Bishop, *Proc. Natl. Acad. Sci. U.S.A.* **80**, 2519 (1983); J. M. Bishop, *Annu. Rev. Biochem.* **52**, 301 (1983).
7. J. M. Coffin, *J. Gen. Virol.* **42**, 1 (1979).
8. M. P. Goldfarb and R. A. Weinberg, *J. Virol.* **38**, 136 (1981).
9. The bands were excised and the ^{32}P was measured by liquid scintillation counting. The background radioactivity was determined separately for each band from a gel fragment immediately above each band. The relative numbers of probe molecules in each band of a given lane were then calculated by correcting the counts per minute in each band for the number of labeled bases in the corresponding probe fragment.
10. K. F. Conklin *et al.*, *Mol. Cell. Biol.* **2**, 638 (1982).
11. The 5′ RNA bands were diminished in the poly(A)$^+$ samples, relative to the other bands, since the 5′ sequences were further from the poly(A) tract and thus recovered during poly(A) selection at lower efficiency.
12. If we assume random distribution of readthrough and normal RNAs in virions, then the composition of genome dimer complexes would be as follows: for wild-type virions, 64% normal-normal, 32% readthrough-normal, and 4% readthrough-readthrough; for mutant virions, 2% normal-normal, 24% readthrough-normal, and 74% readthrough-readthrough.
13. J. Sorge and S. H. Hughes, in *Eucaryotic Viral Vectors,* Y. Gluzman, Ed. (Cold Spring Harbor Laboratory, Cold Spring Harbor, NY, 1982), pp. 127–132; D. A. Foster and H. Hanafusa, *J. Virol.* **48**, 744 (1983).
14. P. A. Norton and J. M. Coffin, *Mol. Cell. Biol.* **5**, 281 (1985).
15. The concentrations of focus-forming units (FFU) were measured in the same culture supernatants from which virion RNA was isolated. The titers were 1.6×10^7 FFU/ml and 2.4×10^7 FFU/ml for M3.14 and M9.13, and 7.3×10^7 FFU/ml and 8.9×10^7 FFU/ml for W10.16 and W10.18, respectively.
16. C.-C. Huang, N. Hay, J. M. Bishop, *Cell* **44**, 935 (1986).
17. R. A. Katz *et al.*, *J. Virol.* **42**, 346 (1982).
18. J. Messing, *Methods Enzymol.* **101**, 20 (1985).
19. T. A. Kunkel, *Proc. Natl. Acad. Sci. U.S.A.* **82**, 488 (1985).
20. Promega Biotec.
21. A. J. Dorner, J. P. Stoye, J. M. Coffin, *J. Virol.* **53**, 32 (1985).
22. S. A. Herman, thesis, Tufts University, Medford, MA (1986).
23. T. Maniatis, E. F. Fritsch, J. Sambrook, *Molecular Cloning: A Laboratory Manual* (Cold Spring Harbor Laboratory, Cold Spring Harbor, NY, 1982), p. 199.
24. We thank T. Henkin and P. Hopper for advice on site-directed mutagenesis and high-performance liquid chromatography. This work was supported by Public Health Service grant CA17659 from the National Cancer Institute.

17 November 1986; accepted 25 February 1987

Formation of Retinal Ganglion Cell Topography During Prenatal Development

BARRY LIA, ROBERT W. WILLIAMS,* LEO M. CHALUPA

A fundamental feature of the mammalian visual system is the nonuniform distribution of ganglion cells across the retinal surface. To understand the ontogenetic processes leading to the formation of retinal ganglion cell topography, changes in the regional density of these neurons were studied in relation to ganglion cell loss and the pattern of retinal growth in the fetal cat. Midway through the gestation period, the density of these neurons was only two to three times greater in the area centralis than in the peripheral retina, whereas shortly before birth this central-to-peripheral difference was nearly 20-fold. Age-related changes in the ganglion cell distribution were found not to correspond in time or magnitude to the massive loss of ganglion cells that occurs during prenatal development. Rather, the formation of ganglion cell density gradients can be accounted for by unequal expansion of the growing fetal retina—peripheral regions expand more than the central region, thereby diluting the peripheral density of ganglion cells to a greater degree. Nonuniform growth, in conjunction with differential periods of neurogenesis of the different types of retinal cells, appears to be a dominant factor regulating overall retinal topography. These results suggest that the differential regional expansion of the fetal retina underlies the formation of magnification factors in the developing visual system.

IN ANIMALS WITH HIGHLY DEVELOPED focal vision the distribution of ganglion cells across the retinal surface is strikingly nonuniform. The density of ganglion cells peaks around the fovea or area centralis—the region of the retina specialized for focal vision—and declines sharply toward the periphery (*1*). This central-to-peripheral gradient in ganglion cell topography dominates retinotopic maps in the visual centers of the brain and is related to variations in measures of acuity across the visual field (*2*).

The development of ganglion cell density gradients poses an intriguing problem because regional specialization in the ganglion cell layer is reflected in the neuronal circuitry throughout the visual system. Early in development the regional distribution of ganglion cells is relatively uniform (*3–5*), and the number of these neurons is much greater in the fetal retina than at maturity (*6, 7*). It has been proposed that differential ganglion cell death across the retina is responsible for the establishment of ganglion cell topography (*3, 8*). This would be the case if during ontogeny greater numbers of ganglion cells die in the peripheral retina than in the central retina. A substantial amount of cell death does occur during development of the mammalian retina. For instance, it has been estimated that in the cat five of six ganglion cells generated during fetal life are eliminated by maturity (*6*). However, it remains to be determined whether such massive loss of neurons contributes significantly to the formation of retinal topography.

An alternative explanation for the establishment of ganglion cell topography is the nonuniform expansion of the growing retina. During ontogeny the growth of the peripheral retina could be greater than that of the central retina, thereby diluting the peripheral population of ganglion cells to a greater degree. Such a pattern of retinal growth has been shown to occur in the postnatal cat (*9*), and this process may also be a key factor in sculpting the distribution pattern of retinal ganglion cells during fetal development.

In this study, we describe developmental changes in the distribution of ganglion cells across the retina of prenatal cats and relate these findings to ganglion cell loss and retinal growth. We show that a primordial area centralis is present early in development and that the progressive increase in the central-to-peripheral gradient in ganglion cell density results primarily from differential expansion of the retina rather than ganglion cell loss.

Ganglion cell topography was examined in fetal cats ranging in age from day 35 of gestation (E35)—just after ganglion cell generation has ended (*10*) and after the initial innervation of retinorecipient nuclei (*11, 12*)—to E62, about 3 days before birth. All surgical procedures were carried out under aseptic conditions with the use of 1 to 2% halothane in oxygen supplemented with 30% nitrous oxide. To identify centrally projecting retinal ganglion cells, 2 to 15 μl of horseradish peroxidase or horseradish peroxidase conjugated to wheat germ agglutinin was injected bilaterally into the posterior thalamus and midbrain or into the optic chiasm. This retrograde labeling procedure was necessary because it is not possible to unequivocally differentiate ganglion cells from other cell types in the ganglion cell

Department of Psychology and the Physiology Graduate Group, University of California, Davis, CA 95616.

*Present address: Section of Neuroanatomy, Yale University School of Medicine, New Haven, CT 06510.

layer with conventional histological procedures. Fetuses were taken by cesarean section 12 to 24 hours later, deeply anesthetized with an intraperitoneal injection of sodium pentobarbital, and perfused with mixed aldehydes. Retinas were removed, cleaned of vitreous humor, reacted to demonstrate peroxidase activity, and flat-mounted on gelatinized slides (*13*). Counts of labeled cells were made at sites distributed at least every 0.5 mm in a grid pattern over the entire retina. The resulting counts were plotted on projection drawings of the retinal whole mount. Essentially all labeled cells were confined to the ganglion cell layer, although a few displaced ganglion cells were observed (*14*).

In every retina, a region situated temporal and superior to the optic disk contained the highest density of labeled ganglion cells (Fig. 1). This region, located along the raphe of the nerve fiber layer, straddled the decussation line separating temporal and nasal hemiretinas (*15*). Precisely these features characterize the adult area centralis.

As an index of developmental changes in the gradient of ganglion cell distribution, we calculated the ratio of labeled ganglion cell densities at the area centralis to that in the retinal periphery. We refer to this value as the central-to-peripheral (C/P) ratio. The peak density was obtained by counting cells in adjacent ocular reticule fields across the entire area centralis until the highest value was found. The peripheral density was determined by averaging counts at sites beyond three-quarters of the distance from the area centralis to the retinal margins. These values are listed in Table 1.

Changes in the C/P ratio as a function of fetal age are shown in Fig. 2. In the youngest retina, E35, this ratio was 2.6:1 (*16*). During the next 2 weeks the ratio rose slowly to 4.7:1 at E48, and thereafter the change in the C/P ratio accelerated so that just before birth it was greater than 18:1.

The relation between the evolving C/P ratio and the normal elimination of retinal ganglion cells in fetal cats is also shown in Fig. 2 (*17*). Most ganglion cells are eliminated between E39 and E52, at a time when there is only a gradual, twofold increase in the C/P ratio. Conversely, relatively few ganglion cells are lost between E52 and E62, a period during which there is an accelerated change in the C/P ratio. Thus, the development of the C/P ratio during fetal life does not correspond in time or magnitude to the loss of retinal ganglion cells.

Although we cannot rule out the possibility that ganglion cell loss may serve to refine retinal topography, this mechanism cannot be the dominant factor responsible for establishing regional specialization in the fetal retina (*18*). Accordingly, we sought to determine whether differential growth of the prenatal retina accounts for the increase in the C/P ratio during prenatal development.

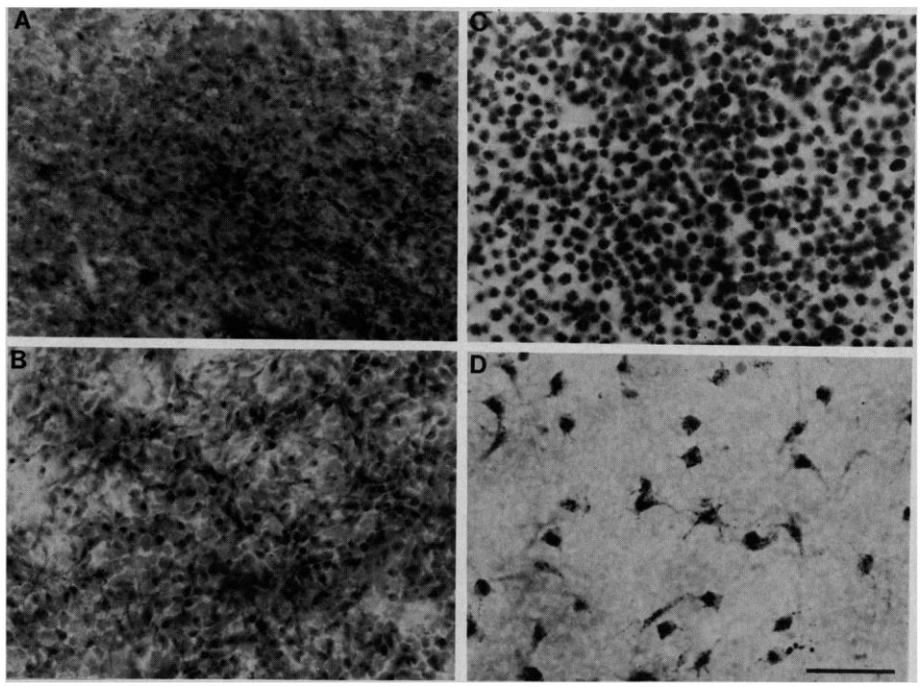

Fig. 1. Photomicrographs showing retrogradely labeled ganglion cells in the flat-mounted retina of the fetal cat at the youngest and oldest ages studied. These micrographs are from the area centralis (**A**) and periphery (**B**) of an E35 retina and the corresponding regions (**C** and **D**) of an E62 retina. Calibration bar, 50 μm.

In the fetal retina there are two clearly identifiable reference points with which to gauge the uniformity of retinal growth, the area centralis and the optic disk. We measured the distance between these two landmarks to obtain a measure of central retinal growth and compared this value to measures of overall retinal expansion—the distances between the area centralis and the nasal, temporal, superior, and inferior margins of the retina. As may be seen in Fig. 3, the distance between the area centralis and the optic disk increased by the lowest factor. These linear measurements demonstrate that the central region of the retina grows substantially less than the peripheral regions of the retina.

If nonuniformity in retinal expansion underlies the formation of regional gradients in the fetal retina, then the increase in the C/P ratio should be directly related to retinal growth. This is indeed the case (Fig. 4). The linear relation between the C/P ratio and retinal area is highly significant (slope = 0.107 ± 0.010; $P < 0.001$), and the deviation of the points about the line is characterized by a standard deviation of 1.43 (*19*). We conclude that nonuniform growth of the fetal retina can satisfactorily account for the formation of ganglion cell topography dur-

Table 1. Labeled ganglion cell densities at the area centralis and in the retinal periphery and the resultant C/P ratios. The increase in the C/P ratio with fetal age is due to the greater reduction of ganglion cell densities in the retinal periphery. There were variations in the number of labeled cells between animals of similar age (for example, E40 to E44, or E56), which is probably due to incomplete labeling of the total ganglion cell population. However, it is improbable that the regional distribution of labeled ganglion cells reflects differential uptake of tracers in the fetal brain. All our injections were sufficiently large to diffuse evenly throughout the target areas. Since the C/P ratios were not affected appreciably by the absolute degree of labeling, this measure provides an appropriate index of regional differences in ganglion cell density in the fetal retina. Furthermore, although the total number of unlabeled cells fluctuated among animals, this measure did not vary systematically as a function of fetal age.

Age	Ganglion cell density (no./mm²)		C/P ratio
	Area centralis	Periphery	
E35	28,828	11,262	2.56
E37	34,202	12,142	2.87
E40	39,577	13,383	2.96
E41	21,499	6,282	3.42
E42	18,567	5,310	3.50
E44	33,225	8,857	3.75
E48	20,521	4,511	4.55
E48	18,078	3,861	4.68
E52	19,544	2,852	6.85
E52	20,033	2,869	6.98
E56	14,658	1,344	10.91
E56	19,056	1,693	11.25
E56	19,056	1,716	11.10
E62	19,544	1,068	18.29

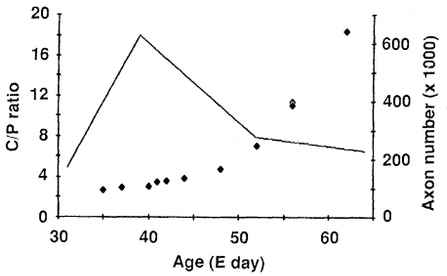

Fig. 2. Changes in the C/P ratio (points) and optic axon number (*6*) (solid lines) as a function of fetal age.

ing prenatal development. Differential expansion of the retina continues postnatally and ultimately results in an additional threefold increase in both retinal area and the C/P ratio (*9*).

The foregoing analysis applies to the overall central-to-peripheral gradient in ganglion cell density. It is likely, however, that nonuniform retinal growth also contributes to more localized regional differences in ganglion cell density. For instance, as in Fig. 3, the temporal quadrant of the retina expands to a greater degree than the nasal quadrant. Correspondingly, there is a greater decrease in ganglion cell density in the temporal periphery than in the nasal periphery (*20*).

Although differential growth is a key factor in the genesis of ganglion cell topography, this mechanism alone cannot be responsible for generating the density distribution of all retinal cell types. Photoreceptors, horizontal cells, bipolar cells, and amacrine cells are each distributed differently across the retina and have gradients less steep than that of ganglion cells (*21*). Even different classes of retinal ganglion cells exhibit distinct C/P ratios (*22*). Such dissimilarities probably reflect the fact that each cell type is generated during a different period of retinal growth (*10, 23*) and is consequently subject to different magnitudes of peripheral dilution (*24*). In accord with this hypothesis, the beta class of ganglion cells is generated during an earlier period than the alpha cell class (*10*) and has a sharper gradient at maturity (*22*).

The present results, as well as those of Mastronarde *et al.* (*9*) on the postnatal retina, clearly show that ganglion cell topography in the cat can be largely accounted for by differential retinal growth. In a recent histological study of the fetal cat retina (*25*) it was suggested that differential growth is an important factor in generating the area centralis, and accumulating evidence from work on other species indicates that differential growth may be a common feature of mammalian retinal development (*26*). At present, however, we have little information on the processes that control such differential retinal expansion. Moreover, a remarkable coordination of growth patterns throughout the eye must operate to properly align the visual axis with regional specializations of the retina. As a first step, it would be important to determine whether retinal growth reflects the proliferation of nonneural elements, the hypertrophy of neurons or interstitial cells, or other factors. Few studies have addressed this fundamental problem (*27*), and as yet it is unknown whether the relevant control factors are intrinsic or extrinsic to the developing retina.

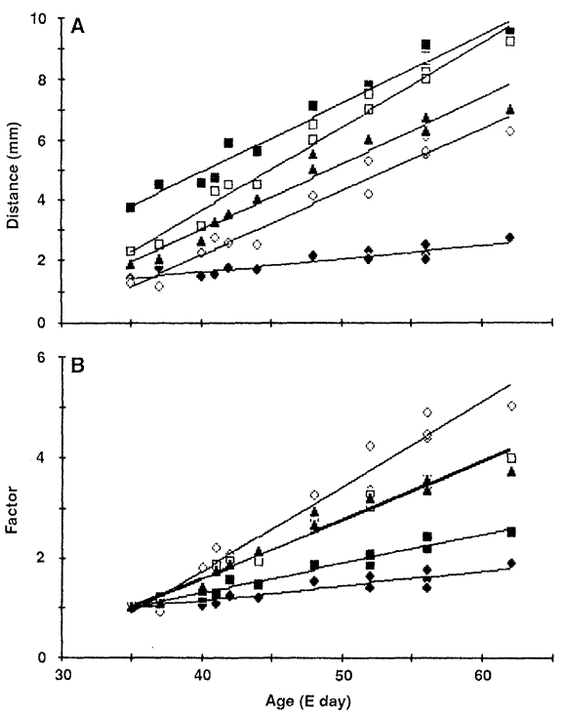

Fig. 3. (**A**) Changes in the absolute distances from the area centralis to the optic disk (◆) and to the temporal (◇), nasal (■), superior (□), and inferior (▲) retinal margins as a function of fetal age. (**B**) These changes expressed as factors of increase from the initial values at E35 (same symbols).

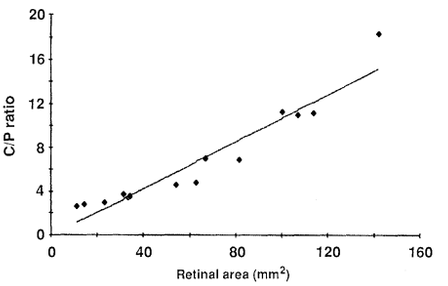

Fig. 4. Changes in the C/P ratio as a function of retinal area. The linear regression equation for this relation is C/P = −0.008 + 0.107(area).

Our findings also have important implications for the formation of retinotopic projections in the developing visual system. Retinal axons innervate their target nuclei before pronounced changes are evident in the C/P ratio (*11, 12*). Moreover, developing retinofugal projections in the cat exhibit a remarkable degree of order, similar to that of the adult (*28*). As a consequence of differential retinal growth, the region of the target nucleus innervated by the peripheral retina will represent a progressively greater proportion of the prospective visual field relative to the region innervated by cells originating from the central retina. Thus, the nonuniform expansion of the prenatal retina is probably a major determinant of the pronounced magnification of the central visual field representation evident in retinotopic maps throughout the visual system.

REFERENCES AND NOTES

1. G. L. Walls, *The Vertebrate Eye and Its Adaptive Radiation* (Hafner, New York, 1942); R. W. Rodieck, *The Vertebrate Retina* (Freeman, San Francisco, 1973); A. Hughes, in *Handbook of Sensory Physiology*, F. Crescitelli, Ed. (Springer-Verlag, Berlin, 1977), vol. 7, part 5, pp. 613–756.
2. S. Polyak, *The Vertebrate Visual System* (Univ. of Chicago Press, Chicago, 1957); J. S. Pointer, *Biol. Rev.* **61**, 97 (1986).
3. J. Stone, D. H. Rapaport, R. W. Williams, L. M. Chalupa, *Dev. Brain Res.* **2**, 231 (1982).
4. B. Lia, R. W. Williams, L. M. Chalupa, *Soc. Neurosci. Abstr.* **9**, 702 (1983).
5. J. M. Provis, F. A. Billson, P. Russell, *Invest. Ophthalmol. Vis. Sci.* **24**, 1316 (1983); J. M. Provis, D. Van Driel, F. A. Billson, P. Russell, *J. Comp. Neurol.* **233**, 429 (1985).
6. R. W. Williams, M. J. Bastiani, B. Lia, L. M. Chalupa, *J. Comp. Neurol.* **246**, 32 (1986).
7. A. Y. Ng and J. Stone, *Dev. Brain Res.* **5**, 263 (1982); P. Rakic and K. P. Riley, *Science* **219**, 1441 (1983); R. W. Williams, M. J. Bastiani, L. M. Chalupa, *J. Neurosci.* **3**, 133 (1983); J. M. Provis, D. Van Driel, F. A. Billson, P. Russell, *J. Comp. Neurol.* **238**, 92 (1985); B. Lia, R. W. Williams, L. M. Chalupa, *Dev. Brain Res.* **25**, 296 (1986).
8. Retinal ganglion cell death has been well documented in the mammalian retina [for example, T. J. Cunningham, I. M. Mohler, D. L. Giordano, *Dev. Brain Res.* **2**, 203 (1982); D. R. Sengelaub and B. L. Finlay, *J. Comp. Neurol.* **204**, 311 (1982)]. It has also been suggested that some ganglion cells are lost during early development as a result of the transformation of immature ganglion cells into amacrine cells [J. W. Hinds and P. L. Hinds, *ibid.* **213**, 1 (1983)]. However, the validity of the transformation hypothesis has been questioned [B. Dreher, R. A. Potts, M. R. Bennett, *Neurosci. Lett.* **36**, 255 (1983); V. H. Perry, Z. Henderson, R. Linden, *J.*

Comp. Neurol. **219**, 356 (1983)]. In the present study, the terms cell death, loss, and elimination are used interchangeably.
9. D. N. Mastronarde, M. A. Thibeault, M. W. Dubin, *J. Comp. Neurol.* **228**, 598 (1984).
10. M. Kliot and C. J. Shatz, *Soc. Neurosci. Abstr.* **8**, 815 (1982); C. Walsh, E. H. Polley, T. L. Hickey, R. W. Guillery, *Nature (London)* **302**, 611 (1983); C. Walsh and E. H. Polley, *J. Neurosci.* **5**, 741 (1985).
11. R. W. Williams and L. M. Chalupa, *J. Neurosci.* **2**, 604 (1982).
12. R. L. Anker, *J. Comp. Neurol.* **173**, 185 (1977); C. J. Shatz, *J. Neurosci.* **3**, 482 (1983); R. W. Williams and L. M. Chalupa, *Neuroscience* **10**, 1249 (1983); L. M. Chalupa and R. W. Williams, in *Advances in Neural and Behavioral Development*, R. N. Aslin, Ed. (Ablex, Norwood, NJ, 1985), vol. 1, p. 1; C. J. Shatz and D. W. Sretavan, *Annu. Rev. Neurosci.* **9**, 171 (1986).
13. A detailed description of our in utero surgical techniques has been provided in previous publications (*6, 11*). Injection parameters were manipulated (horseradish peroxidase versus wheat germ agglutinin conjugated to horseradish peroxidase, with or without 4% dimethylsulfoxide, retinorecipient nuclei versus optic chiasm injection) in order to ascertain to what extent the degree of labeling depended on procedural considerations. Peroxidase activity was demonstrated with a modified protocol based on the use of pyrocatechol and *p*-phenylenediamine [J. S. Hanker, P. E. Yates, C. B. Metz, A. Rustione, *Histochem. J.* **163**, 107 (1977); V. H. Perry and R. Linden, *Nature (London)* **297**, 683 (1982)]. For the purpose of orientation, small cuts were made in the superior retinal margin in situ before dissection.
14. Using differential interference contrast microscopy, we could observe all labeled and unlabeled cell profiles. Cells were considered labeled only if grains of reaction product were visible in the same plane of focus within the cell profile. Counts were made according to Gundersen's rule, correcting for profiles falling on two adjacent edges of the eyepiece reticule [H. J. G. Gundersen, *J. Microsc. (Oxford)* **111**, 219 (1977)].
15. The decussation line was evident after unilateral injections of horseradish peroxidase (*4*) and after injections of different fluorescent tracers into each optic tract.
16. Since there is a trend for ganglion cells in the central retina to be generated earlier than those in the peripheral retina (*10*), this could contribute to the presence of a peak density at E35. Furthermore, some retinal ganglion cell axons are still growing toward their central targets until E40 (*6*), and consequently C/P ratios obtained prior to this age may somewhat overestimate the central-to-peripheral difference in ganglion cell density. However, this overestimation would not appreciably alter the interpretation of our results.
17. The elimination of retinal ganglion cells illustrated in Fig. 2 is based on axon counts in the fetal optic nerve (*6*). The same time course is apparent in the rise and fall of labeled cell densities in the center and periphery, the peripheral density decreasing to a greater degree (Table 1).
18. For discussion of the factors that might underlie the elimination of ganglion cells in the fetal cat, see (*6*) and M. A. Kirby and L. M. Chalupa [*J. Comp. Neurol.* **251**, 532 (1986)].
19. As a first approximation, a linear function, which requires the fewest assumptions, provides a satisfactory fit to the data. The slight curvilinearity apparent in Fig. 4 could be produced by a decelerating rate of growth in the area centralis relative to the rate of peripheral growth. An overestimation of C/P ratios at the youngest fetal ages may also be a factor (*16*).
20. The ratio of nasal to temporal labeled cell densities in the peripheral quadrants of the retina changes from 1:1 at E35 to 1.6:1 at E62.
21. R. H. Steinberg, M. Reid, P. L. Lacy, *J. Comp. Neurol.* **148**, 229 (1973); H. Wässle, L. Peichl, B. B. Boycott, *Proc. R. Soc. London Ser. B* **203**, 269 (1978); M. Schmidt, H. Wässle, M. Humphrey, *Neurosci. Lett.* **59**, 235 (1985); D. I. Vaney, *Proc. R. Soc. London Ser. B* **244**, 475 (1985).
22. A. Hughes, *J. Comp. Neurol.* **197**, 303 (1981).
23. E. H. Polley, C. Walsh, T. L. Hickey, *Invest. Ophthalmol.* (Suppl.) **22**, 114 (1982).
24. H. Wässle and H. J. Riemann, *Proc. R. Soc. London Ser. B* **200**, 441 (1978).
25. S. R. Robinson, *J. Comp. Neurol.* **255**, 50 (1987).
26. Hamster: D. R. Sengelaub, R. P. Dolan, B. L. Finlay, *ibid.* **246**, 527 (1986); rabbit: S. R. Robinson, B. Dreher, G. M. Horsburgh, M. J. McCall, *Soc. Neurosci. Abstr.* **12**, 985 (1986); rat: B. Dreher, R. A. Potts, S. Y. K. Ni, M. R. Bennett, *Neurol. Neurobiol.* **9**, 39 (1984).
27. A. J. Coulombre, *J. Exp. Zool.* **133**, 211 (1956); D. H. Beach and M. Jacobson, *J. Comp. Neurol.* **183**, 603 (1979); *ibid.*, p. 615; *ibid.*, p. 625; L. Liu, W. Halfter, P. G. Layer, *Cell Tissue Res.* **244**, 501 (1986).
28. D. W. Sretavan and C. J. Shatz, *Nature (London)* **308**, 845 (1984); L. H. Ostrach, M. A. Kirby, L. M. Chalupa, *Soc. Neurosci. Abstr.* **12**, 119 (1986); D. W. Sretavan and C. J. Shatz, *J. Comp. Neurol.* **255**, 386 (1987).
29. We thank R. W. Rodieck for critical review of this manuscript. This work was supported by National Institutes of Health–National Eye Institute grant EY03391.

8 December 1986; accepted 25 March 1987

Clonal Restriction Boundaries in *Xenopus* Embryos Shown with Two Intracellular Lineage Tracers

PHILIP SHEARD AND MARCUS JACOBSON

It has been proposed that clonal restriction boundaries develop in *Xenopus* embryos between clones initiated at the 512-cell stage, and that these boundaries result in formation of morphological compartments, each populated by progeny of a group of ancestral cells. Although this hypothesis has gained some acceptance, it has also been criticized because the use of only one cell lineage tracer was not a conclusive test of the hypothesis. However, the critical experiment, an assessment of the extent of mingling between two labeled clones in the same embryo, has now been performed. A model of the proposed arrangement of the ancestral cell groups in the 512-cell embryo predicted that the two clones would remain separate in 49% of cases and intermingle in 51% of cases. In fact, there was a bimodal distribution, in which separation of the clones occurred in 46% of embryos and extensive interclonal mingling was observed in 54%. These results are not compatible with hypotheses in which a unimodal distribution of mingling would be predicted but are consistent with the compartment hypothesis.

THE COMPARTMENT HYPOTHESIS OF *Xenopus* development was proposed as an explanation for observations on the positions of labeled cells in embryos of *Xenopus* after injection of a lineage tracer, horseradish peroxidase (HRP), into single blastomeres at the 2- to 512-cell stages of development (*1, 2, 3*). This hypothesis, which has achieved only partial acceptance to date (*4, 5*), proposes that ancestral cell groups are formed in the embryo at the 512-cell stage, and that cell mingling is subsequently restricted between the progeny of different ancestral cell groups but not among progeny of cells comprising a single ancestral cell group (*1, 3, 6*). As a result of this clonal restriction of cell mingling, the progeny of each ancestral cell group form a separate morphological compartment. Each compartment contains many different cell types. The patterns of histological differentiation and compartmentalization are not congruent (*6*). Evidence in support of the hypothesis comes not only from lineage tracer studies but also from the observation that, when excised and cultured together, cells of different ancestral cell groups are restricted in their ability to intermingle in comparison with the mingling between cells derived from the same ancestral cell group (*7*).

Within the *Xenopus* central nervous system (CNS), seven compartments (three rostral and four caudal), derived from seven ancestral cell groups at the 512-cell stage of

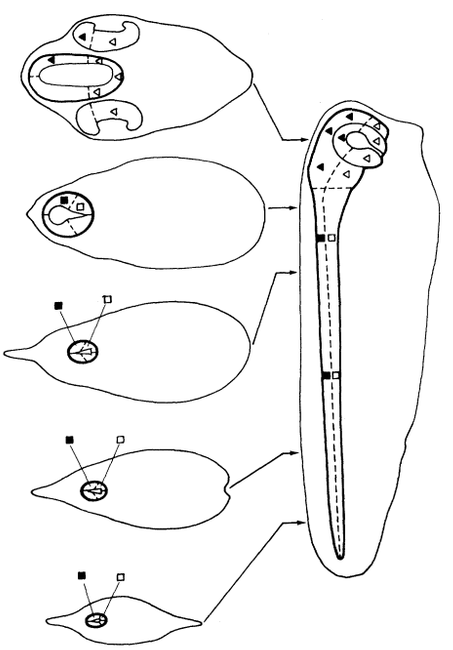

Fig. 1. Diagram of compartments in the central nervous system and retina of tailbud stage *Xenopus* embryo shown in lateral view (**right**) and at five cross-sectional levels (**left**). Compartmental boundaries are shown by dashed lines. Anterior is to the top. Symbols showing compartments on one side only: (▲) anterior-dorsal; (△) anterior-ventral; (■) posterior-dorsal; and (□) posterior-ventral. See text for details.

Anatomy Department, University of Utah School of Medicine, Salt Lake City, UT 84132.